The effect of blanking of TDMA interference on radio-astronomical correlation measurements

Amir Leshem* and Alle-Jan van der Veen
Delft University of Technology, Delft, The Netherlands

ABSTRACT

Radio astronomical observations are increasingly contaminated by man-made communication signals. TDMA signals such as GSM can be suppressed in the time domain by inhibiting the correlation process when the interfering signal is present. In this paper we propose a spectral-temporal detection and blanking scheme applicable to array radio-telescopes. The effectiveness is demonstrated through simulations as well as theoretical analysis.

Keywords: Interference rejection, signal detection, synthesis imaging, radio-astronomical receivers.

1. Introduction

The fast growth of the wireless communication industry poses severe limitations on radio astronomical observations. Two such examples are the Iridium system which will probably cause problems within bands reserved to radio astronomy and the GSM system which became ubiquitous and thus prevents observation in its band. These developments cause an increasing interest in detection and suppression of man-made signals in radio astronomy.

Several methods have been proposed for single dish radio telescopes. A basic approach consists of a single channel power detector used for stopping the integration of the astronomical signal for the duration of the interference. Examples are Friedman's detection of change in the mean power [4], implemented in the RATAN600, and Weber's detector implemented in Nançay [8]. More advanced approaches assume the presence of an additional omni-directional reference antenna which receives a clean copy of the interference. This allows to subtract the interference using LMS-type techniques [2].

The main drawback of such single channel detectors is that they cannot exploit spatial properties of the interference. In synthesis radio telescopes the desired astronomical signals as well as the interference are received by large sensor arrays. In this situation we can perform combined spectral-temporal and spatial processing to detect and remove only those narrow-band slices for periods and in directions in which the interference is present. This type of solution is very well suited to improve radio astronomical observations in the presence of TDMA communication systems such as GSM and Iridium.

In this paper we propose a simple spatio-spectral detection scheme which enables the blanking of narrow-band interference. (Spatial filtering is outside the scope of the present contribution.) We introduce a simplified mathematical model of the problem and present a subband detection scheme. The effect of blanking is analyzed for the case of a single interferer with known spatial signature. The effectiveness of the space-time detection and blanking process is also demonstrated by a simulation.

2. Received signal model

The Westerbork Synthesis Radio Telescope (WSRT), located in the North of The Netherlands, is a linear East-West array consisting of 14 non-uniformly spaced parabolic dishes, each with a diameter of 23 m. The overall aperture is 3 km. Further details about the array geometry and receivers can be found in [1].

A simplified model of the received signals in complex envelope form is

$$x_k(t) = a_k(\theta,\varphi)s(t) + \sum_{i=1}^{q} a_{ki}s_i(t-\tau_{ki}) + n_k(t) \quad (1)$$

where

- $x_k(t)$ is the received signal at the k-th antenna,
- $a_k(\theta,\varphi)$ is the array response at the k'th antenna in a certain look direction (θ,φ).
- $s(t)$ is an astronomical signal of interest (in fact there will be several),
- q is the number of interferers,
- $s_i(t)$ is the i'th interferer at time t,
- τ_{ki} is the relative delay of the i'th signal at the k'th antenna.
- a_{ki} is the attenuation and phase shift of the i'th signal in its path to the k'th antenna and at the receiver.

*Amir Leshem was supported by the NOEMI project of the STW under contract no. DEL77-4476. Email: leshem,allejan@cas.et.tudelft.nl.

- $n_k(t)$ is the system noise at the k'th receiver. We assume that the system noise is temporally and spatially white Gaussian noise with covariance matrix $\sigma^2\mathbf{I}$. Typical SNR at WSRT is −70 dB.

The model in (1) incorporates the fact that the received channels are delayed so as to maintain a constant look direction of the main beam. These delayed signals are processed by the correlator subsystem, which computes a set of spatial correlation matrices $\mathbf{R}(\tau)$ of dimension 14×14, for a set of 512 lags τ. In WSRT $\mathbf{R}(\tau)$ is estimated every 10 ms. The correlation can be described mathematically as

$$\mathbf{x}(t) = [x_1(t),\ldots,x_{14}(t)]^T$$

$$\mathbf{R}(\tau) \;=\; \frac{1}{N}\sum_{k=0}^{N-1}\mathbf{x}(t_0+kT_s)\mathbf{x}^H(t_0+kT_s-\tau)$$

where $T_s = \frac{1}{f_s}$ is the sampling period, and t_0 is the initial sampling time. Note that using the stationarity of the astronomical source this gives an estimate of $\mathrm{E}\{\mathbf{x}(t_0)\mathbf{x}(t_0-\tau)^H\}$. A typical processing bandwidth is 10 MHz, so the sampling rate is 20 MHz. In the current hardware at WSRT these 10 ms correlations are windowed and Fourier transformed to provide a collection of estimates of the spectrum at each pair of antennas. These spectra are averaged further for 10 s or 60 s to provide the system noise reduction crucial for obtaining the astronomical signal, and the results are stored on tape for off-line processing and imaging.

In the presence of temporal and/or spatially non-white interference, the correlation matrices will be corrupted. The detection of such interference is currently done by a simple change-detection of the received power at each entry of $\mathbf{R}(\tau)$ individually, and by off-line inspection. Our objective is to provide a better estimate of the spatial correlation matrices by implementing an on-line multichannel interference detector, and exclude those time-frequency slices in which the interference is dominant. This will work well if the interference is concentrated in frequency and time, as e.g., in Iridium and the GSM system. The same considerations apply to any narrow-band TDMA system.

3. Subband multichannel detection

In view of the results in [6], subband processing is attractive because it enables the use of well-established narrowband techniques. Moreover, it allows to excise only those frequency bands that are contaminated, rather than the complete data set at all frequencies. If the original band is much wider than the interferers, then it also results in increased interference-to-noise ratio in each subband, thus improving the probability of detection. However for wide-band interferers subband processing might cause degradation of detection probability since the correlation between various frequencies is lost.

In this section we propose subband detection methods and analyze their performance.

3.1. Narrowband data model

There are various ways to implement the subband filtering process to reach a narrowband data model. Here, we assume that N consecutive sample vectors $\mathbf{x}(t)$ are partitioned into M partially overlapping blocks of length L. Performing an FFT on each of the blocks, we obtain a new set of data vectors $\tilde{\mathbf{x}}_m(\omega_\ell)$ for $m = 1,\ldots,M$, at discrete frequencies $\omega_\ell = 2\pi f_s\frac{\ell}{L}$, $\ell = 0,\ldots,L-1$. We can now compute covariance matrices $\tilde{\mathbf{R}}(\omega_\ell)$ for each frequency by

$$\tilde{\mathbf{R}}(\omega_\ell) = \frac{1}{M}\sum_{m=1}^{M}\tilde{\mathbf{x}}_m(\omega_\ell)\tilde{\mathbf{x}}_m(\omega_\ell)^H \qquad (2)$$

Windowing can of course improve the quality of the spectral estimates, but we shall not go into details.

The narrowband requirement under which delays can be regarded as phase shifts is in this case $\frac{f_s}{L}\tau_{\max} \ll 1$, where $\tau_{\max}$ is the maximal delay across the array, around 10μs. At $f_s = 20$ MHz, this implies that we need $L \gg 200$ subbands, so that each has a bandwidth less than 100 kHz [6].

Under the narrowband assumption, $s(t-\tau) \leftrightarrow s(\omega)e^{-j\omega\tau}$, and thus the wide-band interferer model in (1) is replaced by a model of the form

$$\tilde{\mathbf{x}}_m(\omega_\ell) = \mathbf{a}(\theta,\phi,\omega_\ell)\tilde{s}(\omega_\ell) \;+\; \sum_{i=1}^{q}\mathbf{a}_i(\omega_\ell)\tilde{s}_{m,i}(\omega_\ell) + \tilde{\mathbf{n}}_m(\omega_\ell) \qquad (3)$$

so that

$$\tilde{\mathbf{R}}(\omega_\ell) \;\simeq\; \mathbf{A}\tilde{\mathbf{R}}_s\mathbf{A}^H + \sigma_\omega^2\mathbf{I} + \tilde{\mathbf{R}}_v$$

where $\mathbf{A} = [\mathbf{a}_1(\omega_\ell) \;\cdots\; \mathbf{a}_q(\omega_\ell)]$ contains the spatial signature vectors, and $\tilde{\mathbf{R}}_s$ is the $q\times q$ interferer sample covariance matrix at frequency ω_ℓ. In the above equation, the contribution of the astronomical sources is collected in the matrix $\tilde{\mathbf{R}}_v$. In future equations on interference excision, this term will be neglected, since is is still extremely weak at 10 ms integration lengths.

3.2. Single channel spectral detector

Before continuing to the multichannel detection scheme, we describe an adaptation to the single channel case. This is of interest to the many single dish radio telescopes which are likely to suffer from TDMA interference without the ability to use the spatial processing described below.

In the single channel case we have a sequence $\tilde{x}_m(\omega_\ell)$ where $m = 1,\ldots,M$ and $\ell = 0,\ldots,L-1$. If the number of spectral channels L is large enough then, for each ℓ, $\tilde{x}_m(\omega_\ell)$ is approximately a complex Gaussian random variable. Without interference, its variance is $\sigma_\omega^2 = \frac{\sigma^2}{L}$ which is assumed to be known.[1] Assuming at most a single interfering source, also complex Gaussian with unknown variance σ_s^2, we obtain the following hypothesis testing problem:

$$\begin{aligned}\mathcal{H}_0:&\quad \tilde{x}_m(\omega_\ell) \sim \mathcal{CN}(0,\sigma_\omega^2)\\ \mathcal{H}_1:&\quad \tilde{x}_m(\omega_\ell) \sim \mathcal{CN}(0,\sigma_\omega^2+\sigma_s^2)\qquad m = 1,\cdots,M\end{aligned}$$

[1] An estimate could be based on adjacent clean subbands.

This is a rather standard problem in detection theory (cf. [5]). A Neyman-Pearson detector turns out to be independent of σ_s^2 and will compare the total received power to a threshold, γ say, deciding $\mathcal{H}_1$ if

$$\frac{1}{\sigma_\omega^2}\sum_{m=1}^{M}|\tilde{x}_m(\omega_\ell)|^2 \;>\; \gamma.$$

Under the above assumptions we can obtain closed form expressions for the probability of false alarm and probability of detection. We obtain that under $\mathcal{H}_0$ (i.e., noise only) the probability of false alarm is given by

$$P_{FA} \;:=\; P\left(\frac{1}{\sigma_\omega^2}\sum_{m=1}^{M}|\tilde{x}_m(\omega_\ell)|^2 > \gamma\,;\,\mathcal{H}_0\right) \quad = \quad Q_{\chi^2_{2M}}(\gamma)$$

where $Q_{\chi^2_{2M}}(\gamma)$ is the tail probability of a χ^2 random variable with $2M$ degrees of freedom. It has a closed-form expression (cf. [5]):

$$Q_{\chi^2_{2M}}(\gamma) \;=\; e^{-\frac{\gamma}{2}}\sum_{k=0}^{M-1}\frac{\left(\frac{\gamma}{2}\right)^k}{k!}$$

Similarly, the probability of detection of an interference at this threshold γ is given by

$$\begin{aligned} P_D \;&:=\; P(\tfrac{1}{\sigma_\omega^2}\textstyle\sum_{m=1}^{M}|\tilde{x}_m(\omega_\ell)|^2 > \gamma\,;\,\mathcal{H}_1) \\ &=\; P\left(\tfrac{1}{\sigma_\omega^2+\sigma_s^2}\textstyle\sum_{m=1}^{M}|\tilde{x}_m(\omega_\ell)|^2 > \tfrac{\gamma}{1+\sigma_s^2/\sigma_\omega^2}\,;\,\mathcal{H}_1\right) \\ &=\; Q_{\chi^2_{2M}}(\tfrac{\gamma}{1+INR_\omega}) \end{aligned} \tag{4}$$

where $INR_\omega = \frac{\sigma_s^2}{\sigma_\omega^2}$ is the interference-to-noise ratio.

3.3. Multichannel detector with known spatial signature

To illustrate the significant performance improvement that is possible with a multichannel detector, we consider now a simple case of a single narrow-band Gaussian interferer with *known* spatial signature vector $\mathbf{a}$ (normalized to $\|\mathbf{a}\|^2 = p$, where p is the number of channels) in white Gaussian noise. Thus we have

$$\begin{aligned} \mathcal{H}_0:&\quad \tilde{\mathbf{x}}_m(\omega_\ell) = \tilde{\mathbf{n}}_m(\omega_\ell) \\ \mathcal{H}_1:&\quad \tilde{\mathbf{x}}_m(\omega_\ell) = \mathbf{a}\tilde{s}_m(\omega_\ell) + \tilde{\mathbf{n}}_m(\omega_\ell)\,, \qquad m = 1,\cdots,M \end{aligned}$$

where $\tilde{\mathbf{n}}_m(\omega_\ell) \sim \mathcal{CN}(\mathbf{0},\sigma_\omega^2\mathbf{I})$ and $\tilde{s}_m(\omega_\ell) \sim \mathcal{CN}(0,\sigma_s^2)$. Thus,

$$\begin{aligned} \mathcal{H}_0:&\quad \tilde{\mathbf{x}}_m(\omega_\ell) \sim \mathcal{CN}(0,\sigma_\omega^2\mathbf{I}) \\ \mathcal{H}_1:&\quad \tilde{\mathbf{x}}_m(\omega_\ell) \sim \mathcal{CN}(0,\sigma_s^2\mathbf{a}\mathbf{a}^H + \sigma_\omega^2\mathbf{I})\,, \qquad m = 1,\cdots,M. \end{aligned}$$

In this case the Neyman-Pearson detector is given by defining $z_m = \mathbf{a}^H\tilde{\mathbf{x}}_m(\omega_\ell)$, computing

$$\frac{1}{p\sigma_\omega^2}\sum_{m=1}^{M}|z_m|^2 \;\equiv\; \frac{M}{p\sigma_\omega^2}\,\mathbf{a}^H\tilde{\mathbf{R}}(\omega_\ell)\mathbf{a}$$

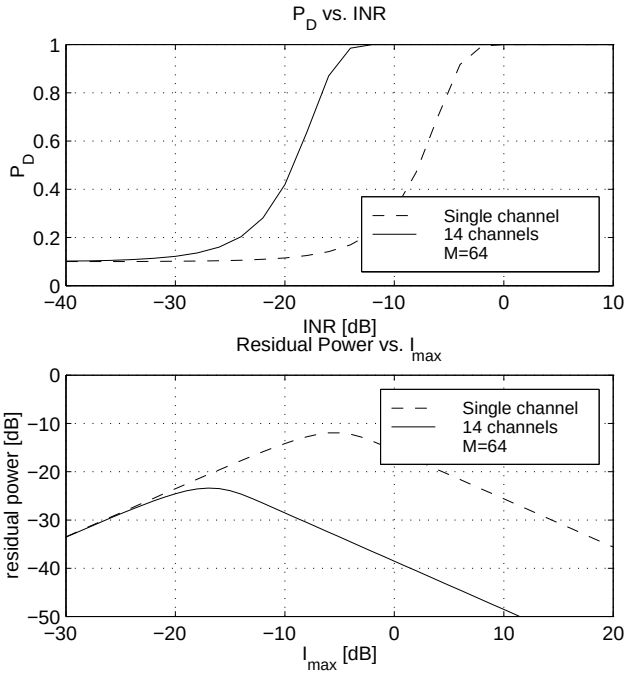

Figure 1. (a) P_D vs. INR. (b) Residual power vs. I_{max}. $M = 64$.

and comparing to a threshold γ. Due to our normalization, taking the same threshold as in the single channel case will provide the same false alarm probability as before. However, the probability of detection is now given by

$$P_D \;=\; Q_{\chi^2_{2M}}(\frac{\gamma}{1+pINR_\omega})$$

Figure 1(a) presents the probabilities of detection as a function of interference to noise ratio for a single and for $p = 14$ channels, and $M = 64$. These are typical numbers for WSRT. We have selected a threshold such that $P_{FA} = 10\%$. We can clearly see the array gain, equal to $10\log(p) = 11.5$ dB.

3.4. Uniform interference in a single block

Now let us consider a case where the INR in a single analysis block of M samples is uniformly distributed in the range $[0, I_{max}]$. The uniform distribution assumption would be appropriate if we look at a single contaminated block, if the detector does not synchronize to the interference and the detection block is of the same length as the maximal block of interference. The expected value of the residual INR, I_{res}, in a single block after detection and blanking is given by

$$I_{res} = \int_0^{I_{max}} I\,(1-P_D(I))\,p(I)\,dI$$

where $p(I) = \frac{1}{I_{max}}(0 \le I \le I_{max})$ is the (uniform) probability of interference. Figure 1(b) presents I_{res} as a function of I_{max}, for the single and 14-channel detectors. We see that the array gain p gives rise to a much greater interference rejection. The effect would be larger for smaller P_{FA}.

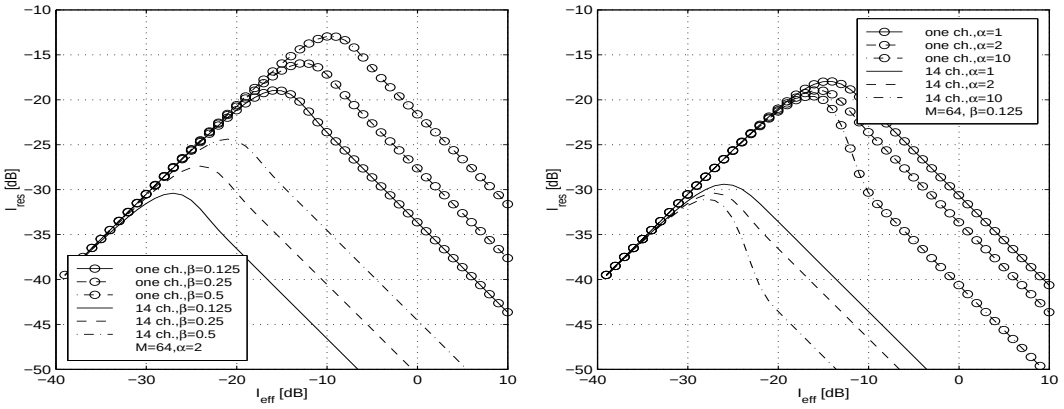

Figure 4. Interference power before and after detection/blanking. (a) Varying duty cycle β; (b) varying slot length α.

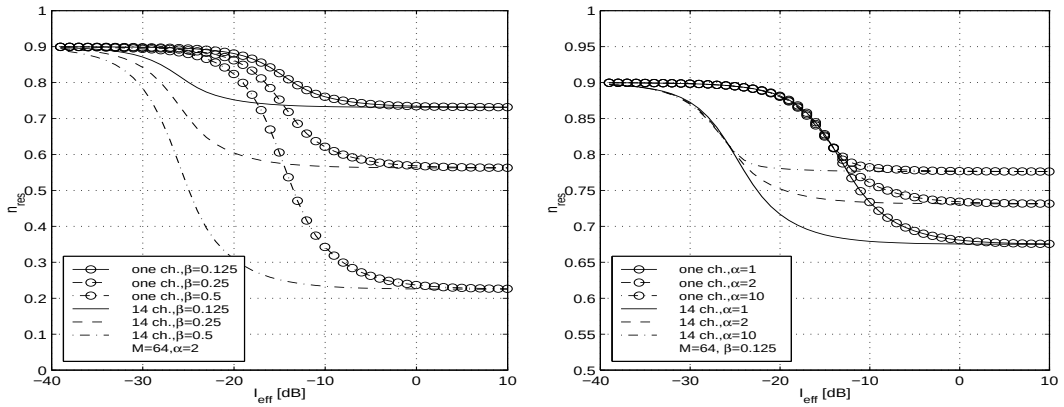

Figure 5. Fraction of kept samples after detection/blanking. (a) Varying duty cycle β; (b) varying slot length α.

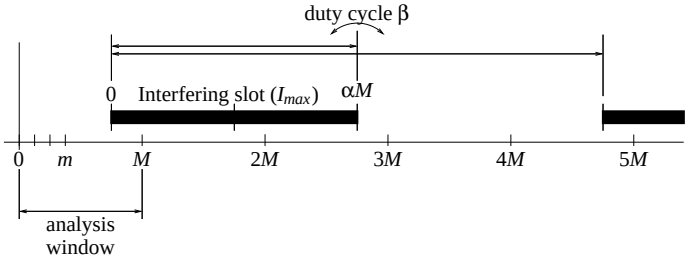

Figure 2. Interferer with slot length αM samples, power I_{max} per on-sample, and duty cycle β.

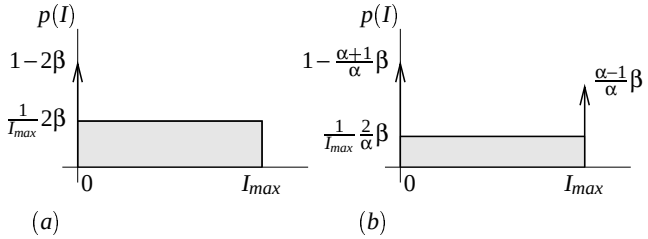

Figure 3. Probability density of interference power in a single analysis window. (a) interference slot length $\alpha = 1$ and duty cycle β; (b) general case.

3.5. Single TDMA interferer with known spatial signature

A more interesting situation occurs if we consider a TDMA signal: an interferer which is periodically active in a fraction β of the time (see figure 2). Here, $0 < \beta < 1$ is known as the duty cycle of the periodic signal. Assume that the interferer is present in a certain frequency band ω_ℓ and that the duration of the slot in which the interferer is active is equal to αM samples $\tilde{\mathbf{x}}_m(\omega_\ell)$, where we take $\alpha > 1$. Let as before I_{max} denote the power of a single sample of the interferer.

The presence of a single interfering slot will now give rise to two analysis windows in which the interferer is partially present, and possibly one or more analysis windows in which the interferer is present in all the samples. Since the interferer is time-slotted with duty cycle β, there will also be windows that contain no interference. The probability density of the interference power in an arbitrary analysis win-

dow of length M is

$$p(I) = \begin{cases} (1-\frac{\alpha+1}{\alpha}\beta)\,\delta(I)\,, & I=0 \\ \frac{1}{I_{max}}\frac{2}{\alpha}\beta\,, & 0<I<I_{max} \\ \frac{\alpha-1}{\alpha}\beta\,\delta(I-I_{max})\,, & I=I_{max} \end{cases}$$

as shown in figure 3(b). Here, $\delta(I)$ is the unit impulse function. This result is readily verified by considering simpler cases such as $\alpha = 1$ (figure 3(a)). We can now define

$I_{eff} = \int I\,p(I)\,dI = \beta I_{max}$
(avg. interference power per sample before detection)

$I_{res} = \int I\,(1-P_D(I))\,p(I)\,dI$
(avg. interference power per sample after det./blanking)

$n_{res} = \int (1-P_D(I))\,p(I)\,dI$
(fraction of number of samples kept after det./blanking)

These functions are illustrated in figures 4 and 5 for varying values of α and β.

4. Multichannel detector with unknown spatial signature

In general, the spatial signature vector **a** of the interference is unknown. Using the matrices $\tilde{\mathbf{R}}(\omega_\ell)$ we can test the hypothesis that there is an interferer in the frequency band ω_ℓ, by detecting the rank of $\tilde{\mathbf{R}}(\omega_\ell)$. In the absence of noise, all eigenvalues of $\tilde{\mathbf{R}}(\omega_\ell)$ will be equal to σ_ω^2, whereas if there are q interferers, then q of those eigenvalues are enlarged by the interferer powers.

If the noise power σ_ω^2 is known, we can apply the likelihood ratio test (LRT), which leads to a method due to Box [3] for testing the null hypothesis that $\sigma_\omega^{-2}\tilde{\mathbf{R}}(\omega_l) = \mathbf{I}$ (no interference). The test statistic is given by

$$-Mp\log\prod(\sigma_\omega^{-2}\lambda_i(\omega_\ell)) \;\sim\; \chi^2_{\frac{(p+1)(p-2)}{2}} \qquad (5)$$

where $\lambda_i(\omega_\ell)$ is the i-th eigenvalue of $\tilde{\mathbf{R}}(\omega_\ell)$.

If also the noise power is unknown, we propose to use the Minimum Description Length (MDL) detector [7]. In this case, rather than setting a threshold based on the asymptotic distribution of the likelihood ratio test (LRT), we try to find the correct model order which minimizes the description length of the data. The MDL rank estimator is given by

$$\hat{k}(\omega_\ell) = \arg\min_k MDL(k,\omega_\ell) \qquad (6)$$

where

$$MDL(k,\omega_\ell) = (p-k)M\log\frac{\frac{1}{p-k}\sum_{i=k+1}^{p}\lambda_i(\omega_\ell)}{\left(\prod_{i=k+1}^{p}\lambda_i(\omega_\ell)\right)^{\frac{1}{p-k}}} + \tfrac{1}{2}k(2p-k+1)\log M$$

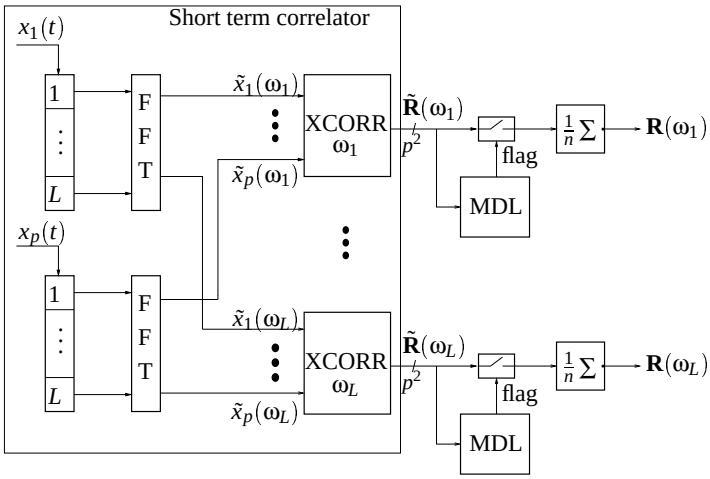

Figure 6. Computational structure of the blanking process

and an interference is detected if $\hat{k} \neq 0$. This rank detector has a simple implementation independent of the varying SINR in the system.

The resulting correlation and detection scheme is depicted in figure 6. For each ω_ℓ the covariance matrix is tested for interference using the MDL criterion. If a decision is made that the covariance matrix is clean the data is passed into a further averaging step, which may typically collect correlation data for 10–30 s.

5. Simulation

In order to show the effectiveness of the blanking process we have generated a very weak sine wave at 400 kHz, arriving from the zenith, together with a frequency hopping GMSK modulated interference. The SNR was –30 dB. The interference was generated as follows: 8 random locations were chosen randomly around the radio-telescope, and to each we have assigned one of five frequencies: 100, 300, 500, 700 and 900 kHz. Every 0.5 ms one of the eight locations was chosen cyclically and a GSM signal with an INR of –10 dB was generated. Its delayed version to each of the radio telescopes (computed by the geometry of the location) were added to the sine wave and the noise.

The spectral estimates were based on $N = 4096$ samples, sampled at 8 MHz, which are approximately 0.5 ms of data. To accelerate computation we have used non-overlapping averaging with $M = L = 64$, so the demonstrated performance can be improved. MDL was used for the detection.

Figure 7 shows the largest eigenvalue of the contaminated covariance matrix, the covariance after blanking was performed and of the signal with no interference present versus frequency. After blanking the sine wave is clearly present. The spectrum shown was based on averaging of 2s of data. The interference was greatly attenuated but not completely removed, due to the missed detection of the interference side-lobes and tails of interfering slots which only partially overlap an analysis block.

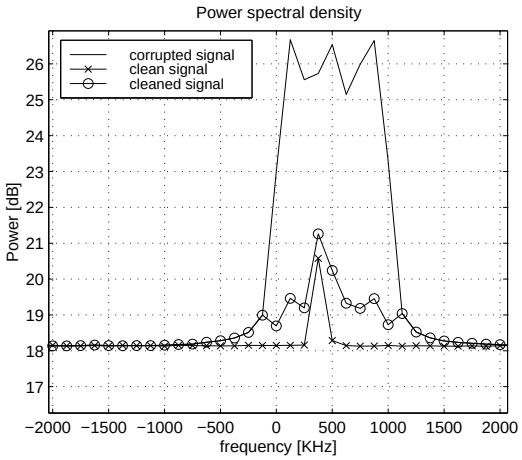

Figure 7. Estimated spectrum before and after blanking

6. Conclusion

Interference detection is greatly improved by employing a multichannel detector. This effect extends beyond the array gain. We have analyzed this for a single TDMA interferer with known spatial signature. Future work will compare the performance of MDL and other detectors to this idealized situation, and assess the trade-off effect of a better detection versus a reduced number of remaining samples. A system for testing the ideas described in the paper is currently being implemented in cooperation with NFRA/ASTRON.

Acknowledgement

We would like to thank our project partners at NFRA especially A. Kokkeler, G. Schoonderbeek, A.J. Boonstra and A. van Ardenne for the very useful collaboration.

7. References

[1] WSRT user documentation. Technical report, NFRA/ASTRON, July 1993.

[2] C. Barnbaum and R. Bradley. A new approach to interference excision in radio astronomy: real-time adaptive cancellation. *The Astronomical Journal*, 115:2598–2614, Nov. 1998.

[3] G. Box. A general distribution theory for a class of likelihood criteria. *Biometrika*, 36:317–346, 1949.

[4] P. Friedman. A change point detection method for elimination of industrial interference in radio astronomy receivers. In *Proc. 8th IEEE Signal Proc. Workshop on Stat. Signal Array Proc.*, pages 264–266, 1996.

[5] S. Kay. *Fundamentals of Statistical Signal Processing. Volume II: Detection Theory*. Prentice Hall PTR, Upper Saddle River, NJ, 1998.

[6] A. Leshem, A. van der Veen, and E. Deprettere. Detection and blanking of GSM signals in radio-astronomical observations. In *Proc. IEEE Signal Proc. Advances in Wireless Comm. (SPAWC99)*, May 1999.

[7] M. Wax and T. Kailath. Detection of signals by information theoretic criteria. *IEEE Trans. Acoust., Speech, Signal Proc.*, 33(2):387–392, Apr. 1985.

[8] R. Weber, C. Faye, F. Biraud, and J. Dansou. Spectral detector for interference time blanking using quantized correlator. *Astronomy and Astrophysics Supplement Series*, 126(1):161–167, Nov. 1997.